Actin Filament Organization in Activated Mast Cells Is Regulated by Heterotrimeric and Small GTP-binding Proteins

James C. Norman,* Leo S. Price,* Anne J. Ridley,§ Alan Hall,‡ and Anna Koffer*

*Physiology Department and ‡MRC Laboratory for Molecular Biology, University College London, London WC1E 6JJ; and §Ludwig Institute for Cancer Research, London W1P 8BT, United Kingdom

Abstract. Rat peritoneal mast cells, both intact and permeabilized, have been used widely as model secretory cells. GTP-binding proteins and calcium play a major role in controlling their secretory response. Here we have examined changes in the organization of actin filaments in intact mast cells after activation by compound 48/80, and in permeabilized cells after direct activation of GTP-binding proteins by GTP-γ-S. In both cases, a centripetal redistribution of cellular F-actin was observed: the content of F-actin was reduced in the cortical region and increased in the cell interior. The overall F-actin content was increased.

Using permeabilized cells, we show that AlF_4^-, an activator of heterotrimeric G proteins, induces the disassembly of F-actin at the cortex, while the appearance of actin filaments in the interior of the cell is dependent on two small GTPases, rho and rac. Rho was found to be responsible for de novo actin polymerization, presumably from a membrane-bound monomeric pool, while rac was required for an entrapment of the released cortical filaments. Thus, a heterotrimeric G-protein and the small GTPases, rho and rac, participate in affecting the changes in the actin cytoskeleton observed after activation of mast cells.

THE activation of cell surface receptors leads to a multiplicity of responses, such as movement, secretion, mitosis, or phagocytosis. Most of these are accompanied by changes in the organization of the cytoskeleton. In secretory cells, such cytoskeletal reorganizations have been suggested to play a role in granule migration and in regulating the access of secretory vesicles to the plasma membrane, as well as endocytotic events after exocytosis (Burgoyne and Cheek, 1985; Linstedt and Kelly, 1987; Sontag et al., 1988).

Cytoskeletal changes after cell activation have been attributed to changes in pH, Ca^{2+} or phosphorylation (Downey and Grinstein, 1989, Del Castillo et al., 1992, Stossel, 1989; Downey et al., 1992) and also to the activation of GTP-binding proteins (Hall, 1992). The latter can work indirectly, via the production of second messengers (such as an increase in Ca^{2+}_i, cAMP, cGMP, or activation of protein kinase C) or via the increased turnover of phosphoinositides, which have been shown to bind to and regulate many actin-binding proteins (Lassing and Lindberg, 1988). However, evidence for direct control of microfilaments by GTPases is accumulating. In electropermeabilized neutrophils, GTP-γ-S was found to induce an increase in F-actin content, even when phospholipase C activity was inhibited (Bengtsson et al., 1990; Therrien and Naccache, 1989). Coronin, an actin-binding protein from *Dictyostelium discoideum*, which accumulates at cell surface projections directed towards the chemoattractant, has sequence similarities with the β subunit of heterotrimeric G-proteins (de Hostos et al., 1991). These β subunits have also been found to be associated with the cytoskeleton of mouse lymphoma cells (Carlson et al., 1986). More recently, microinjection studies with cultured fibroblasts showed that two *ras*-related small GTPases, rho and rac, are essential for the assembly of stress fibres and membrane ruffles, respectively (Ridley and Hall, 1992; Ridley et al., 1992).

GTP-binding proteins are central to the mast cell exocytotic apparatus. Extensive studies of permeabilized mast cells led to a postulation of a GTP-binding protein, G_E, which acts downstream to second messenger production and may be an integral part of the membrane fusion mechanism (Cockcroft et al., 1987). Its nature, however is still unclear and it is now becoming apparent that a number of GTPases, both heterotrimeric (Lillie and Gomperts, 1993; Aridor et al., 1993) and small (Bar-Sagi and Gomperts, 1988; Oberhauser et al., 1992), may be involved.

In this paper, we examine the response of the actin cytoskeleton to stimulation of intact mast cells with compound 48/80, a basic secretagogue that probably activates GTP-binding proteins directly, in a receptor-independent manner (Mousli et al, 1990; Aridor et al., 1990). We compare these responses with those of streptolysin-O (SL-O)[1]

Address correspondence to Dr. Anna Koffer, Physiology Department, University College London, University Street, London WC1E 6JJ, United Kingdom. The current address for Dr. James C. Norman is The Physiological Laboratory, Downing Street, Cambridge CB23EG, United Kingdom.

1. *Abbreviations used in this paper*: CB, chloride buffer; GB, glutamate buffer; GB-EGTA, GB containing 3 mM Na-EGTA; NAD, nicotinamide adenine dinucleotide; PBSME, PBS containing 2 mM $MgCl_2$ and 3 mM Na-EGTA; RP, rhodamine phalloidin; SL-O, streptolysin-O.

permeabilized cells to GTP-γ-S. We find that a net centripetal redistribution of F-actin, observed after the activation of intact cells, could be mimicked simply by addition of GTP-γ-S to permeabilized cells in the absence of Ca^{2+} (pCa > 9). This effect results from a disassembly of the cortex and a de novo polymerization of actin in the cell interior. Using the permeabilized cell system to study these steps separately, we show that an AlF_4^--sensitive heterotrimeric GTPase is involved in the disassembly of the cortical F-actin. In addition, we have examined the effects of two small GTPases, rho and rac, both of which have been implicated in the control of the cytoskeleton (see above), and show that both of them are required for the appearance of F-actin in the interior of the cell.

Materials and Methods

Materials

All nucleotides (GTP-γ-S, GTP, and ATP) were obtained from Boehringer Mannheim Biochemicals (Indianapolis, IN). SL-O was from Murex Diagnostics Ltd., Dartford, United Kingdom (cat. no. MR16, Lot K 809810). V14rhoA, V12racl, and N17racl proteins were purified as GST fusion proteins, subsequently cleaved and characterized as described (Ridley et al., 1992). Glass Multitest slides were from ICN-Flow. [^{32}P]nicotinamide adenine dinucleotide (NAD) (30 Ci/mmol, 2 mCi/ml) was from NEN-Du Pont (Boston, MA). C3 transferase purified from *clostridium botulinum* was a kind gift of Dr. Klaus Aktories (Rudolph-Buchheim-Institute fur Pharmacologie, Giessen, Germany). All other reagents were obtained from the Sigma Chemical Co. (Poole, Dorset, United Kingdom).

Cell Preparation and Treatment

Preparation of rat peritoneal mast cells was as described previously (Cockcroft et al., 1987). The cells, in a solution containing 137 mM NaCl, 2.7 mM KCl, 1.0 mM $CaCl_2$, 2 mM $MgCl_2$, 5.6 mM glucose, 1 mg·ml^{-1} BSA, and 20 mM Na-Pipes, pH 6.8 (chloride buffer [CB]), were allowed to attach to glass Multitest slides (6-mm diameter wells) for 1 h at room temperature. Intact cells were stimulated with 5 μg·ml^{-1} of compound 48/80 in CB for 2 min at 30°C and were then fixed for 20 min with 3.8% formaldehyde in phosphate-buffered saline containing 2 mM $MgCl_2$ and 3 mM Na-EGTA (PBSME). To permeabilize the attached cells, the CB was exchanged for 137 mM Na-glutamate, 2 mM $MgCl_2$, 1 mg·ml^{-1} BSA, 20 mM Na-Pipes, pH 6.8 (glutamate buffer [GB]), and the cells were then exposed for 8 min to streptolysin-0 at 0.4 IU·ml^{-1} in GB containing 3 mM Na-EGTA (GB-EGTA) at room temperature. Permeabilized cells were then washed free of soluble components and excess SL-O with GB-EGTA. 10 min after SL-O addition, cells were treated for 15 min with 30 μM GTP-γ-S (or AlF_4^-, or 2 μg·ml^{-1} V14rhoA or 2 μg·ml^{-1} V12racl) in GB-EGTA at 30°C and then fixed. The 15-min incubation is sufficient to ensure the completion of the secretory response (Koffer, 1993).

AlF_4^- was obtained by addition of 30 mM NaF and 10 μM $AlCl_3$ to glutamate buffer in the absence of EGTA (chelation of the aluminum ions with EGTA or EDTA rendered the fluoride treatment ineffective). The unbuffered calcium levels (~1 μM), resulting from the omission of EGTA at this stage, did not affect the cytoskeleton, provided that the cells were initially permeabilized in the presence of the chelator. To obtain recombinant V14rhoA or V12racl in the GTP form, the proteins (73 μg·ml^{-1}) were incubated with 100 μM GTP in 50 mM Tris containing 5 mM EDTA, pH 7.0, for 20 min, followed by the addition of 10 mM $MgCl_2$. Controls were exposed to the appropriate final concentrations of GTP, Tris, or EDTA (2.7 μM, 1.4, and 0.1 mM, respectively). V14rhoA was active only in the GTP form, prebinding of the protein with GDP rendered it inactive. 0.1 μg·ml^{-1} C3 transferase was added at the time of permeabilization in the presence of 0.5 mM NAD^+, maintained throughout the wash, and removed just before the addition of GTP-γ-S (i.e., 10-min treatment). N17racl was also included with the SL-O and wash at a concentration of 8 μg·ml^{-1}, but was additionally maintained throughout the incubation with GTP-γ-S. 10 μM cytochalasin E was added 3 min after permeabilization and was maintained throughout treatment with GTP-γ-S or V14rhoA.

Freely soluble ATP would be expected to leak from SL-O-permeabilized cells. However, to ensure ATP depletion, in some experiments, the cells were metabolically inhibited. This was achieved by incubation of the attached cells with 6 mM 2-deoxyglucose and 10 μM antimycin A in GB at 37°C for 7 min before the addition of SL-O.

F-actin Staining Protocols

Postlabeling. Total cellular F-actin was visualized by staining-fixed cells for 15 min with 0.6 μM rhodamine phalloidin (RP) in PBSME containing 80 μg·ml^{-1} lysophosphatidyl choline (L-4129; Sigma Chemical Co.).

Prelabeling. To follow the movement of existing F-actin filaments, the cells were labeled before the addition of GTP-γ-S: 4 min after permeabilization, either 0.18 or 2.0 μM RP in GB-EGTA was added. The stain was thoroughly washed off 2 min before the addition of GTP-γ-S (i.e., 4-min exposure to RP). After the usual 15-min exposure to GTP-γ-S, the cells were fixed as described above.

Pre (2.0 μM RP)- and Postlabeling. This protocol was performed to stabilize the F-actin cortex before the addition of GTP-γ-S and then to visualize any additional F-actin formed after the treatment with the nucleotide. The cells were prelabeled with 2.0 μM RP, and the stain washed off as for prelabeling. GTP-γ-S was added for 15 min, and the cells fixed and restained with RP as for postlabeling.

Microscopy and Flow Cytometry

Fixed and stained cells were mounted in PBSME (no glycerol was used because this can lead to cell collapse) and fluorescent images were obtained using a confocal laser scanning microscope (Leica Inc., Deerfield, IL) attached to a microscope (Fluovert-FU; E. Leitz, Inc., Rockleigh, NJ). Excitation was at 514 nm, and emission was >590 nm. Digital images (equatorial optical slices) are displayed using the Leica "glow" look-up table. The equatorial plane of focus was defined as the midpoint between the top and the bottom of the cell. The nucleus usually, but not always, lies on this plane.

Image Analysis

F-Actin Content. F-actin content was determined as a mean of the total pixel RP intensity per equatorial slice ($n > 50$) and related to the appropriate control level. This was confirmed by an "extended focus" method: an image stack was obtained, encompassing the entire depth of the cell, by superimposition of ~20 optical slices, each 1 μm apart, along the cell's z axis. The relative increase in F-actin content after 48/80 or GTP-γ-S treatment obtained by this method was not significantly different from that obtained by the analysis of the area of equatorial slices. No accumulation of F-actin was apparent at the level of cell attachment or at any other plane. Flow cytometric determinations of cellular F-actin content were performed on suspended RP-stained cells as described previously (Koffer et al., 1990).

F-Actin Distribution. Images of equatorial slices were quantified by radial line scan analysis (as shown in Fig. 4). Three lines were obtained per cell for a total of ≥50 cells and the RP fluorescence intensity profiles for each set of experimental conditions were pooled and averaged to form a mean profile. Data obtained from these scans were further analyzed to obtain bar charts (see Figs. 5 and 7). The cortical and the interior regions were designated as regions encompassed by pixel numbers 1–10 and 11–30, respectively. These represent distances of 0–2.45 and 2.45–7.35 μm from the cell edge. Changes in the RP staining of these two regions were calculated as percentages of the total RP intensity in both regions from appropriate control cells (i.e., the sum of intensities of pixels 1–30). The nucleus was normally >8 μm from the cell edge and, therefore, not included in this analysis.

Leakage of F-Actin

Mast cells were attached to 13-mm diameter glass coverslips (at a density of 2×10^8 cells·mm^{-2}) placed within 15-mm wells and permeabilized as described above. At various times after the addition of SL-O, the permeabilizing solution was aspirated from the attached cells. The supernatant and cells were added to sample buffer (Laemmli, 1970) and boiled for 5 min. Determination of actin in these extracts was by SDS-PAGE, followed by densitometry of silver-stained gels as described previously (Koffer and Gomperts, 1989).

[^{32}P]ADP Ribosylation with C3 Transferase

Cells were attached and permeabilized as described above for leakage of ac-

tin. In addition, 4.5 μCi [^{32}P]NAD/well (0.5 μM) and 0.1 $\mu g \cdot ml^{-1}$ C3 transferase were included in the permeabilization buffer. At various times, this supernatant (containing the bulk of the radioactivity) was discarded, and the remaining cells were extracted with the sample buffer and analyzed by a 15% SDS-polyacrylamide gel (Laemmli, 1970). The gel was dried, and labeled proteins were visualized using phosphor-imaging plates and Bio-Imaging Analyzer FUJIX BAS1000 (Fuji, Tokyo, Japan).

The proportion of soluble rho was determined in suspended cells. Mast cells in CB were preincubated on ice with SL-O (0.8 $IU \cdot ml^{-1}$) for 5 min (no permeabilization occurs at this temperature), centrifuged at 4°C, and then resuspended in aliquots (250,000 cells in 200 μl) in GB containing 1 mM phenyl-methylsulphonyl fluoride, 10 $\mu g \cdot ml^{-1}$ leupeptin, 10 $\mu g \cdot ml^{-1}$ pepstatin, 1 mM EDTA, 1 mM EGTA, and 0.5 mg $BSA \cdot ml^{-1}$. Permeabilization was initiated by incubating the cells at 30°C, and samples were withdrawn after 10 and 30 min and centrifuged (1 min at 12,000 *g*). The pellets were resuspended in 200 μl of the above buffer, and both supernatants and pellets were incubated for 20 min at room temperature with C3 transferase (0.1 $\mu g \cdot ml^{-1}$) and 3.7 μCi [^{32}P]NAD (2.5 μM). Proteins were then precipitated by addition of 25 μl 100% trichloroacetic acid (30 min on ice), pelleted (2 min at 1,200 *g*), 2× washed with ethanol-ether (1:1), dissolved in 50 μl of sample buffer, and analyzed as above.

Results

Response of Intact Cells to Compound 48/80

RP staining of quiescent mast cells revealed F-actin to be present primarily at the cortex (Fig. 1 *A*). After stimulation of intact mast cells by compound 48/80, this pattern changed (Fig. 1 *B*): the staining of the cell cortex was now less intense, while that of the cell interior became stronger. There was a marked (~30%) overall increase in the total F-actin

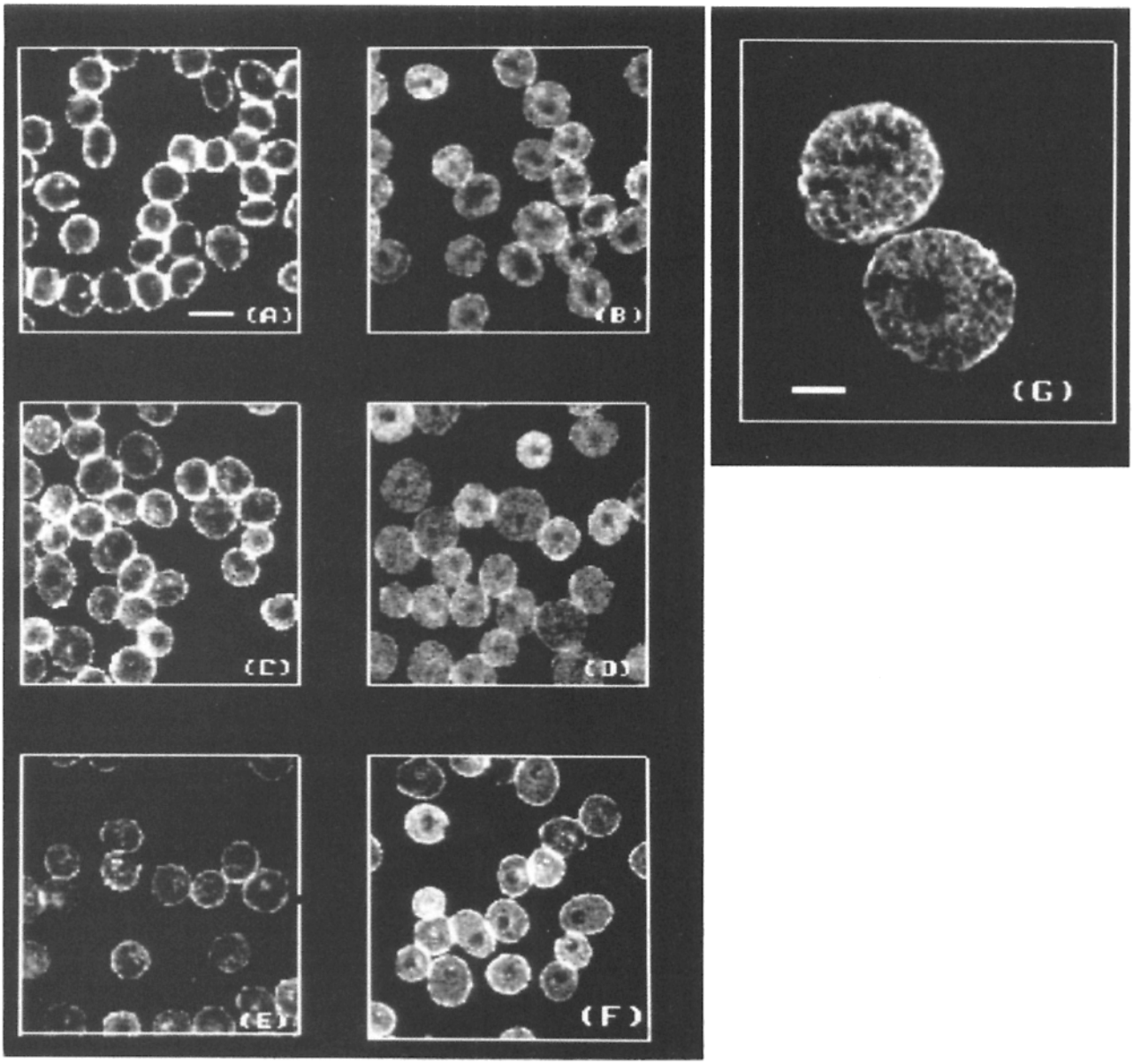

Figure 1. Confocal micrographs of rhodamine phalloidin-stained mast cells showing F-actin distribution in (*A*) unstimulated and (*B*) 48/80-treated intact mast cells. (*C*) Unstimulated and (*D*) GTP-γ-S-treated, permeabilized cells showed similar patterns. Different patterns were exhibited by permeabilized cells treated with (*E*) AlF_4^- and (*F*) V14rhoA. (*G*) shows the internal structures obtained after treatment with GTP-γ-S at higher magnification. The bars in *A* and *G* represent 20 and 10 μm, respectively.

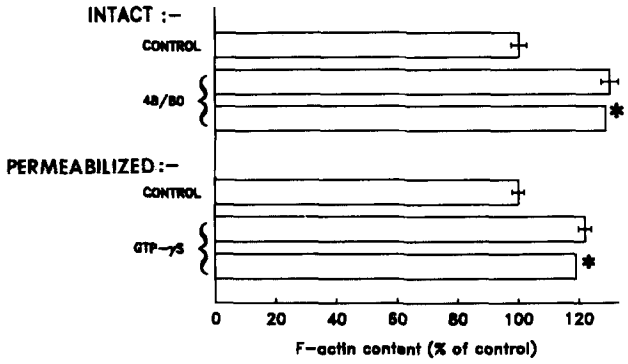

Figure 2. Relative F-actin content of intact and permeabilized mast cells after treatment with compound 48/80 and GTP-γ-S. Values were obtained by quantification of individual cells from confocal images similar to those in Fig. 1 and expressed as percentage of control. The bars with asterisks (*) show confirmation of these values by flow cytometry. Values obtained from confocal imaging are mean ± SEM, $n > 50$ cells. Each asterisked bar represents the mean of two experiments, each involving ≥5,000 cells.

content (Fig. 2), as measured by confocal microscopy or flow cytometry.

Leakage of Actin from Streptolysin-permeabilized Cells

In the experiments described below, cells attached to glass slides were permeabilized by addition of SL-0 (0.4 IU·ml^{-1}) and washed to remove any endogenous ions, nucleotides, and freely soluble components (Koffer, 1993). To establish the proportion of actin remaining within these cells, we determined the extent and time course of actin leakage. Fig. 3 shows that 70–80% of total cellular actin leaked out after permeabilization, and that this process was complete within 4–8 min. Subsequent washing of permeabilized cells did not remove any further actin (not shown). The strong cortical staining of F-actin was not reduced after the permeabilization (compare Fig. 1 *a* and *c*), indicating that the leakage is caused by the diffusion of actin monomers rather than loss of filaments after cytosol dilution. This is consistent with previous results obtained with mast cells in suspension (Koffer et al., 1990) and with other cell types (Cassimeris et al., 1990), which show that the cortical F-actin is very resistant to depolymerization despite the removal of the soluble G-actin pool.

Response of Permeabilized Cells to GTP-γ-S

GTP-γ-S was introduced into washed permeabilized cells 10 min after the addition of SL-O, when only a negligible fraction of the (freely diffusable) G-actin pool remains within the cells. The Ca^{2+} concentration was clamped below 1 nM by EGTA. As shown in Figs. 1 *D* and 2, addition of this nucleotide was sufficient to produce changes in the actin cytoskeleton indistinguishable from those induced in intact cells by 48/80. In spite of the extensive leakage of the monomer, F-actin content increased by ~23% and 19% as measured by confocal microscopy and flow cytometry, respectively (Fig. 2). Higher magnification of cells stimulated by GTP-γ-S (Fig. 1 *G*) or 48/80 (not shown) showed internal structures that appear as if the intergranular cytoplasmic space has been filled with polymerized actin. Identical changes were also obtained in experiments where the interval between the permeabilization and the addition of GTP-γ-S was longer (≤20 min).

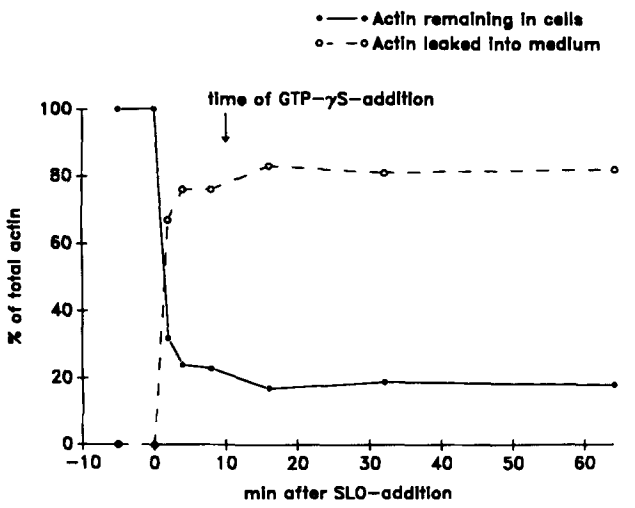

Figure 3. Time course of actin leakage from SL-O-permeabilized mast cells. Cells were attached onto glass coverslips. The actin remaining within the attached cells and that leaking into the supernatant was determined at various times after the addition of streptolysin-O (0.4 IU·ml^{-1}) and plotted as a percentage of total cellular actin content. Determination of actin was by SDS-PAGE, followed by densitometry of silver-stained gels. The time at which GTP-γ-S was routinely added to the incubation (to perform experiments presented in Figs. 1, 3, 4, and 5) is shown by the arrow.

No ATP was required for this response. To confirm this, we have depleted the endogenous ATP content by a pretreatment of cells with metabolic inhibitors, deoxyglucose and antimycin A, before permeabilization. Exposure of these cells to GTP-γ-S produced similar results (data not shown). Furthermore, to exclude the participation of protein kinase C, we have also treated the cells with a protein kinase C inhibitor, H7 (100 μM, added at the time of permeabilization and maintained throughout GTP-γ-S treatment) (Kawamoto and Hidaka, 1984). Again, there was no significant effect on the response.

Quantitative Analysis of Changes in F-Actin Distribution

Changes in the distribution of F-actin after the stimulation of intact and permeabilized cells were further analyzed. Images, such as those shown in Fig. 1, were quantified by radial line scan analysis of equatorial slices, and the RP fluorescence intensity profiles for each set of experimental conditions were pooled. The cortical and the interior regions were designated as regions encompassed by pixel numbers 1–10 and 11–30, respectively. These represent distances of 0–2.45 and 2.45–7.35 μm from the cell edge (Fig. 4 *B*). The nucleus was normally >8 μm from the cell edge and, therefore, not included in this analysis. Fig. 4 *A* confirms and quantifies the effects of GTP-γ-S seen in Fig. 1 *D*: a selective decrease and increase of F-actin presence in the cortical and the internal regions, respectively. Very similar scans were obtained for stimulated intact cells.

Data obtained from these scans were expressed in the form of a bar chart shown in Fig. 5. Changes in the regions designated as cortical (*full bar*) and internal (*hollow bar*) were calculated as percentages of the total F-actin content in both

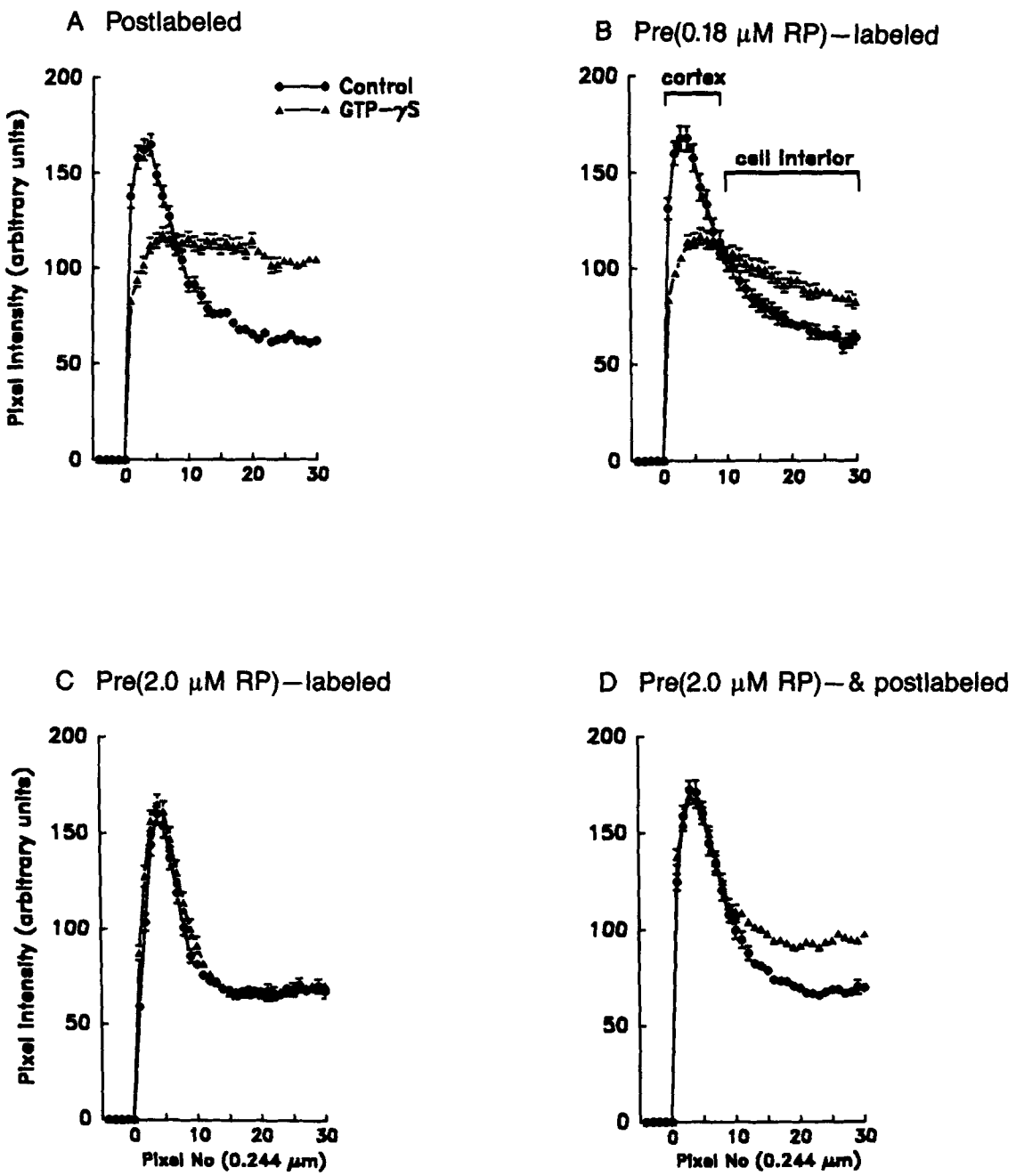

Figure 4. Changes in the F-actin distribution induced by GTP-γ-S in permeabilized cells. Densitometric line scan analyses were performed on confocal images similar to those in Fig. 1. Three radial scan lines were obtained per cell, each extending from the exterior to the center of the cell. The intensity profiles of these lines were pooled to form a mean profile ± SEM, $n > 50$ cells. (*A*) Postlabeled: the distribution change in actin filaments after the treatment with GTP-γ-S. The cells were stained with RP after fixation to visualize all the F-actin present. (*B*) 0.18 μM RP prelabeled: the component of the distribution change resulting from the relocalization of cortical actin filaments to the cell interior. Cells were permeabilized in the presence of 0.18 μM RP, which was then removed before the addition of GTP-γ-S. (*C*) 2.0 μM RP prelabeled: stabilization of the actin cortex by preincubation of the cells with 2.0 μM RP prevented GTP-γ-S–induced relocation of cortical filaments to the cell interior. (*D*) 2 μM RP prelabeled and postlabeled: the component of the distribution change resulting from the newly polymerized filaments in the cell interior. This was obtained by using the treatment shown in (*C*) followed by that shown in (*A*). Relocalization of actin was prevented by prelabeling the permeabilized cells with 2 μM RP. The cells were then treated with GTP-γ-S and postlabeled.

regions from appropriate control cells (the sum of intensities of pixels 1–30). Thus, relative changes in distribution of F-actin induced by GTP-γ-S could be easily evaluated (Fig. 5, *group II, first pair*): a reduction in the cortical region of ~10% and an increase in the interior region of ~30%. Similar changes were produced by compound 48/80 in intact cells, except that the increase in the cell interior region was slightly greater (Fig. 5, *group I*).

The Fate of the Cortical Filaments

To examine the fate of existing filaments, the cells were

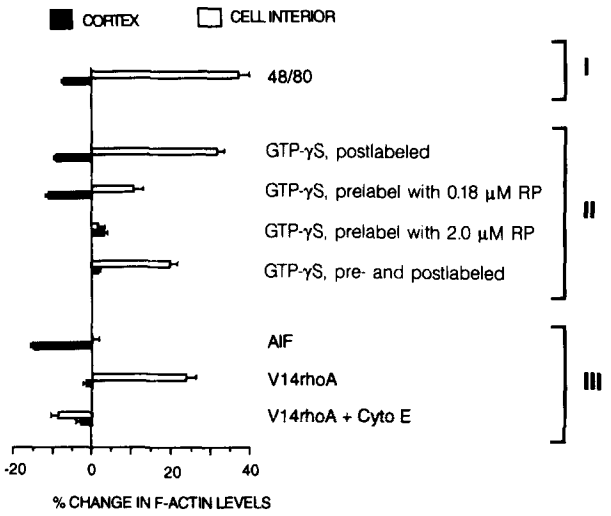

Figure 5. Changes in the levels of F-actin in the cortical (*full bars*) and the interior (*hollow bars*) regions of the cell, expressed as percentages of the total F-actin content in both regions of appropriate control cells. Data were extracted from densitometric scans similar to Fig. 4 by integration of areas under the traces designated as cortex and cell interior, respectively. Values are mean ± SEM, $n > 50$ cells. (*I*) The effect of compound 48/80 on intact cells. (*II*) The effect of GTP-γ-S on permeabilized cells. These four pairs represent an analysis of the data shown in Fig. 4 (*A–D*). (*III*) AlF_4^- and V14rhoA effects on the levels of F-actin in the cortical and the interior regions, respectively, are different and independent. The inhibitory effect of cytochalasin E on V14rhoA-induced polymerization of F-actin is also shown.

stained with a low (0.18 μM) concentration of RP shortly after permeabilization, but before the exposure to GTP-γ-S (prelabeling). Subsequent addition of GTP-γ-S caused a relocation of these prelabeled filaments (Fig. 4 *b*), such that the increase in the intensity of the cell interior paralleled the loss from the cortex (Fig. 5, *group II, second pair*). This GTP-γ-S–induced redistribution of the filaments was completely prevented when the concentration of the prelabeling RP was increased to 2.0 μM, nearer to the saturating concentration of RP for F-actin (Faulstich et al., 1988) (Figs. 4 *c* and 5, *group II, third pair*).

De Novo Actin Polymerization

To compare the contributions of the newly polymerized and the relocated filaments in the cell interior, the following experiment was performed. We used a combination of prelabeling by 2 μM RP (to prevent the relocalization of the cortical filaments as in Fig. 4 *c*), followed by stimulation with GTP-γ-S and then further labeling with 2 μM RP (to label any newly formed filaments). The appearance of new filaments occurred exclusively in the cell interior (Figs. 4 *d* and 5, group II, *fourth pair*). Thus, both relocation of cortical filaments and de novo actin polymerization contribute to the increase in the internal staining.

Effect of Cytochalasin E

The distribution change shown in Fig. 4 *a* seems to result from disassembly of cortical F-actin combined with movement of filaments from the cortex to the cell interior, together with a de novo polymerization of actin from a G-actin pool that is apparently retained within permeabilized cells. However, it is also possible that previously "hidden" filaments (such as would have been inaccessible to RP) become accessible to RP after GTP-γ-S treatment. We have tested the effects of cytochalasin E, a microfilament-destabilizing agent that blocks filament barbed ends (Cooper, 1987). This agent prevented the GTP-γ-S induced overall increase in F-actin content (not shown), indicating de novo actin polymerization from newly exposed barbed ends rather than exposure of hidden RP-binding sites.

Activation of Heterotrimeric G Proteins by AlF_4^- Causes Cortical Disassembly

GTP-γ-S affects the activity of both heterotrimeric and small, ras-related, GTP-binding proteins. To differentiate between the contributions of these two classes, we first tested the effects of AlF_4^-, a specific activator of trimeric G-proteins (Kahn, 1991). Treatment of permeabilized cells with AlF_4^- led to selective loss of cortical F-actin (Figs. 1 *e*; 5, *group III*). This indicates that a heterotrimeric G-protein is directly involved in disassembly of the actin cortex. However, no increase in F-actin in the cell interior was observed. Thus, activation of this AlF_4^- sensitive G-protein was not sufficient to relocate cortical filaments to the cell interior neither could it induce the de novo actin polymerization. Activity of additional GTP-binding proteins must, therefore, be required for the entrapment of the released filaments and for the de novo actin polymerization.

A Substrate for the C3 Transferase is Present in Permeabilized Mast Cells

Members of the rho family of GTP-binding proteins are the most obvious candidates for the above roles. These proteins are substrates for the C3 transferase from clostridium botulinium. This enzyme inactivates rho proteins by ADP ribosylation (Aktories et al., 1989). To test for the presence of rho family proteins, mast cells were permeabilized with SL-O in the presence of C3 transferase and [^{32}P]NAD for varying lengths of time. The radioactive proteins remaining in the cells were then visualized by SDS-PAGE followed by phosphor imaging. The results (Fig. 6) show one major radioactive band at 20 kD, the ribosylation of which reached a maximum after 10 min of incubation with C3. No ribosylation was evident in the absence of the toxin.

To establish the proportion of soluble and membrane-bound rho, leakage experiments were performed on cells in suspension. Results are shown in Table I. Only ~40% of C3 substrate (the 20-kD band) was found to leak out of the cells after their permeabilization, and the leakage was complete within 10 min. Using a recombinant rho protein as a standard, ~0.85 ng ± 0.4 ($n = 3$) of rho (total) was calculated to be present per 100,000 cells. This represents ~0.3 μM rho, when extrapolated to intact cells (cell volume is ~1.3 × 10^{-12} liters).

Rho Induces Polymerization of Actin in the Cell Interior

Having established the presence of rho proteins remaining within mast cells after permeabilization, the constitutively active recombinant V14rhoA mutant (Ridley and Hall, 1992; Ridley et al., 1992) was used to investigate any involvement

Figure 6. Ribosylation of rho by C3 transferase. Attached mast cells were permeabilized with SL-O in the presence of C3 transferase and [^{32}P]NAD. After the indicated times, the cell supernatant was removed, and radioactive proteins remaining within the cells were analyzed by SDS-PAGE and phosphor-imaging. Lanes *2–5* show treatment with C3 for 20, 15, 10, and 5 min, respectively. A protein of ~20 kD is ribosylated in a time-dependent fashion, reaching a maximum after 10–15 min. Lane *1* shows that no radioactive bands are obtained in the absence of C3.

of this small GTPase in the cytoskeletal response of mast cells. Introduction of V14rhoA into SL-O–permeabilized cells promoted an increase in F-actin content of the cell interior with no significant decrease of F-actin in the cortical region (Figs. 1 *f* and 5, *group III*). This response is identical to that obtained by treatment of cells as described in Figs. 4 *d* and 5, *group II* (GTP-γ-S, pre- and postlabeled). V14rhoA was only active in the GTP form, prebinding of the protein with GDP rendered it inactive (not shown). In the presence of cytochalasin E, the rho-induced increase in F-actin content was completely inhibited (Fig. 5, *group III*).

Table I. Leakage of C3 Transferase Substrate from Permeabilized Mast Cells

	PSL	Percentage (P+S)
10 min		
Pellet (P)	4,893	56
Supernatant (S)	3,901	44
P+S	8,794	
30 min		
Pellet	5,985	62
Supernatant	3,691	38
P+S	9,676	
Unfractionated		
Total	8,317	

ADP-ribosylation with [^{32}P]NAD was performed as described in Materials and Methods. Proteins were separated by SDS-PAGE (100,000 cells/lane) and analyzed by a Bio-Imaging Analyzer. Results are expressed as phosphosensitive luminescence intensity obtained from appropriate bands (PSL, background subtracted).

Rho is not Required for Relocalization of Cortical Filaments

Fig. 7 shows changes induced by the addition of GTP-γ-S in the presence of various agents. These changes are shown in two ways: (*a*) the overall F-actin distribution change ("post"), which is the sum of the filament disassembly, relocalization, and the de novo actin polymerization (as determined by post-labeling experiments described in Fig. 4 *a*); and (*b*) the change caused by the filament relocalization only ("pre," as determined by prelabeling experiments described in Fig. 4 *b*). Inhibition of rho by C3, or blocking of barbed ends by cytochalasin E, produced identical effects. In the presence of either of these agents, GTP-γ-S failed to induce an increase in cellular F-actin content. However, the relocalization of cortical filaments to the cell interior was unaffected, showing that the nucleation sites activated by rho are not responsible for entrapment of filaments, liberated from the cortical region by the AlF_4^--sensitive G-protein. In some experiments, C3 and cytochalasin caused a fall in the resting levels of F-actin. The reduction, however, was never >20%, and

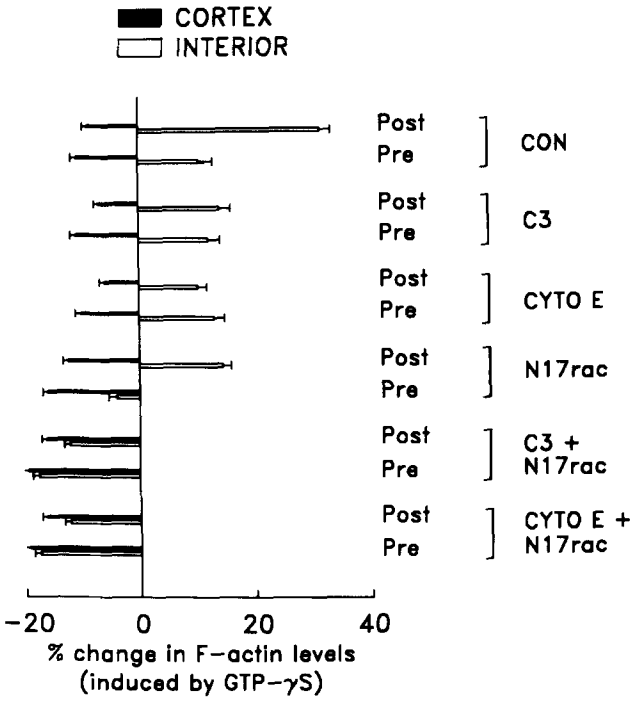

Figure 7. The effect of various agents on GTP-γ-S–induced change in the F-actin content and filament relocalization,. Changes in the cortical and the interior regions of the cell are shown by full and hollow bars, respectively. The data are presented in the same fashion as Fig. 5. F-actin movement is demonstrated by following the redistribution of (0.18 μM) RP-prelabeled filaments (*PRE*), overall F-actin content changes (i.e., filament movement plus de novo polymerization) by postlabeling the cells (*POST*) with RP. GTP-γ-S causes both relocalization and de novo polymerization. C3 transferase and cytochalasin E have no effect on filament relocalization, but they completely abolish de novo polymerization. Conversely, N17rac1 completely blocks the entrapment of prelabeled filaments within the cell interior, but does not significantly reduce the de novo polymerization. N17rac1 added together with either C3 or cytochalasin leads to a large, GTP-γ-S–induced fall in cellular F-actin content.

it became less apparent after increasing the time between permeabilization and the addition of these agents.

Inhibition of the Activity of rac by N17rac1 Prevents Filament Relocalization

Since neither heterotrimeric G-proteins nor rho were involved in filament relocalization, we tested the role of rac, a rho-related protein. N17rac1 has been used previously in microinjection studies as a dominant negative inhibitor of rac (Ridley et al., 1992). Fig. 7 shows that addition of this protein to permeabilized cells completely blocks GTP-γ-S–induced filament redistribution from the cortex to the cell interior. Using the prelabeling protocol, the cortical staining was reduced by addition of GTP-γ-S, but there was no commensurate increase in cell interior staining. This indicates that rac is required for the entrapment of the released cortical filaments within the cell interior. De novo actin polymerization, however, was unaffected by N17rac1 because a considerable increase in internal staining was still detected by the postlabeling protocol (Fig. 7). In addition, N17rac1 did not affect the basal levels of cellular F-actin (not shown). No changes in the cytoskeleton were observed upon addition of the constitutively active form of rac, V12rac1 (not shown). It appears that in the absence of cortical actin disassembly, no relocalization of filaments can occur.

Inhibition of both rho and rac Causes GTP-γ-S–dependent Loss of Filaments

Since the activities of rho and rac are required for actin polymerization and filament entrapment, respectively, it follows that inhibition of both processes together should cause a reduction in total cellular F-actin content in response to GTP-γ-S. Fig. 7 shows that this is in fact the case. In the presence of N17rac together with either C3 or cytochalasin E, addition of GTP-γ-S leads to a significant loss of F-actin from the cell (both of pre- and postlabeled filaments). This is similar to the situation observed after the addition of AlF_4^- to permeabilized cells (Fig. 5, *group III*). In both cases, presumably, there is no filament entrapment or actin polymerization because rho and rac are not activated.

Discussion

GTP-binding Proteins Regulate Mast Cell Microfilaments Independently of Freely Soluble Cytosolic Components

We show here that GTP-binding proteins play a major role in the cytoskeletal reorganization that accompanies mast cell activation. Two changes in F-actin morphology were elicited by the exposure of permeabilized cells to GTP-γ-S: the disassembly of the cortex and the appearance of actin filaments in the cell interior. Released cortical filaments, as well as newly polymerized actin, were recruited into this interior cytoskeleton. These effects result (at least in part) from the GTP-γ-S activation of two small GTPases, rho and rac, and of a heterotrimeric G-protein(s).

GTP-γ-S–induced reorganization of actin proceeded in the absence of any freely soluble cytosolic components, indicating that the GTP-binding proteins and any accessory proteins must be associated with intracellular structures and remain within mast cells for ≥10 min after SL-O permeabilization. This is supported by our finding that the inhibitors of both rho and rac had profound effects on the response of the permeabilized cells. These results are somewhat unexpected because in the presence of Mg^{++}, the binding of GTP-γ-S to small GTPases requires a nucleotide exchange protein (Downward, 1990; Hall, 1993; Takai et al., 1992). Exchange proteins specific for rho and rac have not been identified so far (Hiraoka et al., 1992). The exchange factor for a small GTPase ras, sos, has been found to be translocated from the cytosol to the plasma membrane upon activation of a tyrosine kinase receptor, resulting in a formation of a multiprotein complex that includes the activated ras (Egan et al., 1993). Sos, however, does not leak from quiescent cells when they are permeabilized with SL-O (Downward, J., personal communication). Using cell fractionation studies, rac has been found to be cytosolic in quiescent neutrophils, and to translocate to the plasma membrane upon exposure of the cells to activating stimuli, again participating in the formation of a complex of the NADPH-oxidase system (Abo et al., 1991; Quinn et al., 1993). Similarly, thrombin activation of platelets resulted in an increased association of rho with cytoskeletal fractions (Zhang et al., 1993). We have found the major part (~60%) of rho (as a C3 substrate) to be associated with internal structures of (resting) mast cells (Table I). It is possible that small GTPases and their exchange factors are loosely associated with the appropriate membrane, adjacent to their effectors. Signals, which activate the cell, would then merely consolidate this association and promote the assembly of a multiprotein complex.

Since freely soluble endogenous nucleotides have also been removed during the permeabilization and washing procedures, and no exogenous ATP is required, it is unlikely that a phosphorylation event constitutes an integral part of the GTP-γ-S–induced response. Moreover, neither depletion of ATP before the addition of SL-O (by incubating cells with metabolic inhibitors) nor treatment of permeabilized cells with H7, an inhibitor of protein kinase C (Kawamoto and Hidaka, 1984), affected the response. However, addition of MgATP enhanced the proportion of permeabilized cells that responded to GTP-γ-S, and it caused an increased F-actin presence in the cell interior (data not shown).

It is interesting to note that the centripetal rearrangements of the mast cell cytoskeleton occurred in the absence of Ca^{2+}. Previous results have shown that Ca^{2+} introduced into permeabilized mast cells, can cause a substantial loss of F-actin content independently of GTP-γ-S (Koffer et al., 1990). Thus, it appears that two routes to cytoskeletal regulation, one independent of and the other dependent on Ca^{2+}, operate in mast cells and most probably interact and modify each other. The absence of Ca^{2+}, ATP, and the cytosolic factors would exclude the involvement of most second messengers, but a G-protein–induced change in phospholipid composition may well mediate some of these effects. In this context, recent evidence for the activation of both phosphatidylinositide 3-kinase (Zhang et al., 1993) and phospholipase D (Bowman et al, 1993) by rho related protein may be relevant.

Disassembly of Cortical Microfilaments

AlF_4^- treatment of permeabilized mast cells could mimic one aspect of the GTP-γ-S–induced response. It resulted in a selective decrease of cortical F-actin, indicating a presence

of an heterotrimeric G-protein that regulates disassembly of cortical actin filaments and/or their detachment from the plasma membrane. Higher (> μM) concentrations of RP protected the cortical filaments from both GTP-γ-S or AlF_4^--induced disassembly. Thus, a calcium independent, phalloidin-sensitive and membrane-associated, actin-severing protein may be involved. A possible candidate is actin depolymerizing factor, whose severing activity is inhibited by phalloidin (Maciver et al., 1991) and regulated by phosphoinositides (Yonezawa et al., 1990), and whose association with plasma membrane has previously been demonstrated (Koffer et al., 1988).

The response of neutrophils to both GTP-γ-S and AlF_4^- has been studied previously and found to be somewhat different from that of mast cells. In electropermeabilized neutrophils, AlF_4^- and GTP-γ-S both caused an increase in F-actin content (Therrien and Naccache, 1989; Bengtsson et al., 1990). This may be caused by the much smaller lesions in electropermeabilized cells, which result in the retention of the bulk of the monomeric G-actin pool and cytosolic components.

De Novo Actin Polymerization in the Cell Interior

The appearance of new filaments in the cell interior was partially reproduced by addition of V14rhoA to permeabilized cells. Newly polymerized filaments appeared despite the loss of soluble actin. New filament formation was sensitive to cytochalasin E and, therefore, dependent on the presence of free filament barbed ends. The implications of this are important, suggesting the existence of a membrane-bound (or slow-leaking) G-actin pool that can be readily mobilized when actin polymerization is required. Thus, rho may initiate the release of this sequestered G-actin together with the formation of new actin nucleation sites.

Recent evidence suggests that such membrane-associated G-actin pool may well exist (Herman, 1993; Cao et al., 1993). This sequestered pool of G-actin could represent a ready-to-go pool of monomer stored where it is most needed, near the advancing edge of a migrating cell. The increase in F-actin content of mast cells was quantitatively similar, regardless of whether the cells were intact or permeabilized. This suggests that the same membrane-bound pool of G-actin may also be recruited after activation of intact cells by 48/80.

Examination of the high magnification micrograph (Fig. 1 *G*) suggests that actin polymerization after exposure to GTP-γ-S (or V14rhoA) occurs on the secretory granule membranes which may, therefore, be the location of rho in these cells. Indeed, C3 substrates on purified neutrophil granule membranes have already been identified (Philips et al., 1991). The role of rho in stress fiber production has been postulated to be via stabilization of a multiprotein complex, components of which are recruited from the cytosol, creating focal adhesion from which the fibers emanate (Ridley and Hall, 1992). In mast cells, the F-actin, which was seen to form around secretory granules, may also originate from multiprotein complexes that may provide new (cytochalasin sensitive) nucleation sites. However, in mast cells, the components of such a complex must already be associated with the appropriate (internal) membranes because they are resistant to leakage after permeabilization.

Relocalization of Cortical Filaments

In the presence of GTP-γ-S, disassembled cortical filaments did not leave permeabilized cells, and they were redistributed to their interior (Fig. 5, *group II*). On the other hand, after the AlF_4^- treatment, the filaments were lost from cells (Figs. 1 *E* and 5, *group III*), presumably because of their depolymerization into monomers and/or short oligomers and leakage. The experiments using N17rac1 suggest that activation of rac is required to entrap the filaments within the cell interior. This entrapment was unaffected by C3 exoenzyme or cytochalasin E, and thus does not involve rho nor a barbed end-on polymerization event. The mechanism of this presumably rac-dependent entrapment is unknown; a side-on or a pointed end-on (cytochalasin insensitive) association of the filaments with internal membranes and/or actin may be responsible. Rac may also act to stabilize the released cortical filaments, preventing their depolymerization. A number of actin-associated proteins are known to bind to the sides of F-actin, for instance tropomyosin, α-actinin and actin-binding protein, which can act to stabilize the filaments or promote parallel and othogonally cross-linked arrays of actin, respectively (Pollard and Cooper, 1986). Rac activity has been shown to be necessary for the formation of membrane ruffles in fibroblasts (Ridley et al., 1992). Membrane ruffles are rich in F-actin, which is extensively cross-linked. The role of rac in fibroblasts may be not only to initiate actin polymerization, but also to stabilize and cross-link filaments within ruffles while reducing the rigidity of the cortex.

No effect was observed following the introduction of an activated rac (V12rac1) into permeabilized cells. This is most probably caused by the absence of cortical actin disassembly and, therefore, the absence of any filaments to be relocalized. In addition, no freely soluble pool of actin monomer is present in permeabilized cells, such as may have been required for the formation of ruffles in fibroblasts.

Conclusions

Treatment of intact cells with compound 48/80 produced changes in microfilament morphology, which were very similar to those induced by GTP-γ-S in permeabilized cells: a centripetal rearrangement of F-actin. The similarity of these responses supports the evidence for a direct (i.e., receptor-independent) activation of heterotrimeric G-proteins by compound 48/80 and other basic secretagogues (Mousli et al., 1990; Aridor et al., 1990, 1993). To transduce signals from this 48/80-sensitive, plasma membrane–associated, heterotrimeric G-protein to rho and rac in the cell interior, we postulate the existence of a cytosolic factor(s). This is illustrated in the scheme shown in Fig. 8. These cytosolic components would be lost from permeabilized cells, and this may be the reason why the AlF_4^- effect is limited only to the cortical disassembly.

We conclude that a heterotrimeric G-protein releases filaments from the cortex, which are then trapped within the cell by a rac-dependent mechanism. In addition, rho mobilizes a membrane-associated G-actin pool and mediates polymerization of actin in the cell interior. Together, these three activated GTP-binding proteins can induce centripetal rearrangements of the mast cell cytoskeleton independently of Ca^{2+}.

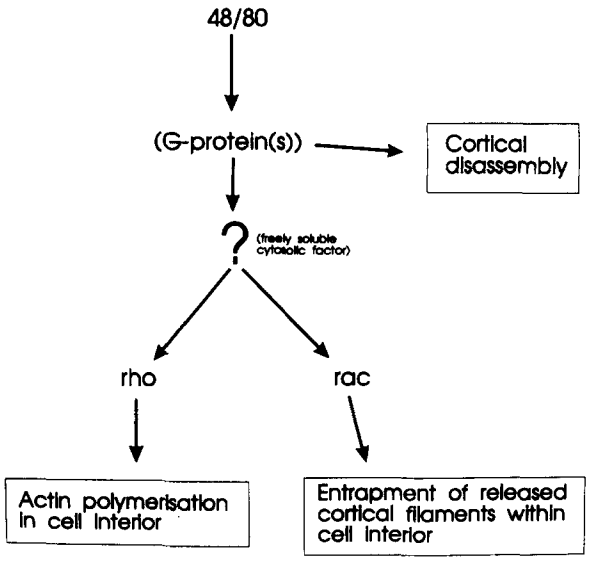

Figure 8. Scheme for regulation of the actin cytoskeleton in mast cells. Compound 48/80 activates a heterotrimeric G-protein(s) situated on the plasma membrane, which is directly involved in cortical disassembly. In turn, this G-protein(s) communicates with granule-associated rac and rho via a diffusable cytosolic factor. Active rho then promotes de novo actin polymerization in the cell interior by mobilizing a membrane-bound monomeric pool and providing new barbed end nucleation sites, and rac mediates entrapment of the released cortical filaments. When mast cells are permeabilized, the soluble factor leaks from the cell, thus disconnecting the heterotrimeric G-protein from rho and rac. The three GTP-binding proteins are then activated directly by GTP-γ-S.

Centripetal movement of actin filaments is a phenomenon that has been reported in many cell types and accompanies cellular processes such as locomotion or pseudopodial extensions (Heath, 1983; Theriot and Mitchison, 1992). This study provides a quantitative insight into another example of such movements in model secretory cells. The relevance of these cytoskeletal changes to the exocytotic process remains to be established. Since GTP-γ-S-induced exocytotic fusion is fully inhibited by 1 mM GDP-β-S (Koffer, 1993), whereas inhibition of cytoskeletal changes requires higher (10 mM) concentrations (not shown), the G-protein(s) postulated to control exocytosis in mast cells, G_E (Cockcroft et al., 1987), cannot be responsible for this type of cytoskeletal redistribution. This study is, however, consistent with the postulate that cortical disassembly is a necessary preliminary step for secretion (Burgoyne and Cheek, 1985; Linstedt and Kelly, 1987). Possible roles for internal filaments, on the other hand, could be to provide a structural support for degranulating cells and to restrict granule movement, thus tempering any uncontrolled secretory response.

We would like to thank Prof. M. Whittaker and Dr. S. Bolsover for the use of the confocal microscope that was purchased with funds from the Wellcome Trust, and Dr. K. Aktories for providing the C3 transferase.

This work was supported by grants from The Medical Research Council and The Wellcome Trust. A. Hall is supported by the Cancer Research Campaign and the Medical Research Council.

Received for publication 27 December 1993 and in revised form 17 May 1994.

References

Abo, A., E. Pick, A. Hall, N. Totty, C. G. Teahan, and A. W. Segal. 1991. Activation of the NADPH oxidase involves the small GTP-binding protein $p21^{rac1}$. *Nature (Lond.).* 353:668–670.

Aktories, K., S. Braun, S. Rosener, I. Just, and A. Hall. 1989. The rho gene product expressed in *E. coli* is a substrate for botulinum ADP-ribosyltransferase C3. *Biochem. Biophys. Res. Commun.* 158:209–213.

Aridor, M., G. Rajmilevich, M. A. Beaven, and R. Sagi-Eisenberg. 1993. The heterotrimeric G-protein G_{i3} stimulates final steps in regulated exocytosis. *Science (Wash. DC).* 262:1569–1572.

Aridor, M., L. M. Traub, and R. Sagi-Eisenberg. 1990. Exocytosis in mast cells by basic secretagogues: evidence for direct activation of GTP-binding proteins. *J. Cell Biol.* 111:909–917.

Bar-Sagi, D., and B. D. Gomperts. 1988. Stimulation of exocytotic degranulation by microinjection of the *ras* oncogenic protein into rat mast cells. *Oncogene.* 3:463–469.

Bengtsson, T., E. Sarndahl, O. Stendahl, and T. Andersson. 1990. Involvement of GTP-binding proteins in actin polymerization in human neutrophils. *Proc. Nat. Acad. Sci. (USA).* 87:2921–2925.

Bowman, E., D. Uhlinger, and J. Lambeth. 1993. Neutrophil phospholipase D is activated by a membrane-associated rho family small molecular weight GTP-binding protein. *J. Biol. Chem.* 268:21509–21512.

Burgoyne, R. D., and T. R. Cheek. 1985. Reorganization of peripheral actin filaments as a prelude to exocytosis. *Biosci. Rep.* 7:281–288.

Cao, L-G., D. Fishkind, and Y. L. Wang. 1993. Localization and dynamics of nonfilamentous actin in cultured cells. *J. Cell Biol.* 123:173–181.

Carlson, K. E., M. J. Woolkalis, M. G. Newhouse, and D. Manning. 1986. Fractionation of the β subunit common to guanine nucleotide-binding regulatory proteins with the cytoskeleton. *Mol. Pharmacol.* 30:463–468.

Cassimeris, L., H. McNeill, and S. H. Zigmond. 1990. Chemoattractant-stimulated polymorphonuclear leukocytes contain two populations of actin filaments in their spatial distributions and relative stabilities. *J. Cell Biol.* 110:1067–1075.

Cockcroft, S., T. W. Howell, and B. D. Gomperts. 1987. Two G-proteins act in series to control stimulus-secretion coupling in mast cells: use of neomycin to distinguish between G-proteins controlling polyphosphoinositide phosphodiesterase and exocytosis. *J. Cell Biol.* 105:2745–2750.

Cooper, J. A. 1987. Effects of cytochalasin and phalloidin on actin. *J. Cell Biol.* 105:1473–1478.

de Hostos, E. L., B. Bradtke, F. Lottspeich, R. Guggenheim, and G. Gerisch. 1991. Coronin, an actin binding protein of *Dictyostelium discoideum* localized to cell surface projections, has sequence similarities to G protein β subunits. *EMBO (Eur. Mol. Biol. Organ.) J.* 10:4097–4104.

Del Castillo, A., M. Vitale, and J.-M. Trifaro. 1992. Ca^{2+} and Ph determine the interaction of chromaffin cell scinderin with phosphatidylserine 4,5,-biphosphate and its cellular distribution during nicotinic-receptor stimulation and protein kinase C activation. *J. Cell Biol.* 119:797–810.

Downey, G., C. Chan, P. Lea, A. Takai, and S. Grinstein. 1992. Phorbol ester-induced actin assembly in neutrophils: role of protein kinase C. *J. Cell Biol.* 116:695–706.

Downey, G., and S. Grinstein. 1989. Receptor-mediated actin assembly in electropermeabilized neutrophils: Role of intracellular pH. *Biochem. Biophys. Res. Commun.* 160:18–24.

Downward, J. 1990. The ras superfamily of small GTP-binding proteins. *Trends in Biochem. Sci.* 15:469–472.

Egan, S., B. W. Giddings, M. Brooks, L. Buday, A. Sizeland, and R. Weinberg. 1993. Association of Sos Ras exchange protein with Grb2 is implicated in tyrosine kinase signal transduction and transformation. *Nature (Lond.).* 363:45–51.

Faulstich, H., S. Zobeley, G. Rinnerthaler, and J. V. Small. 1988. Fluorescent phallotoxins as probes for filamentous actin. *J. Musc. Res. Cell Motil.* 9:370–383.

Hall, A. 1992. Ras-related GTPases and the cytoskeleton. *Mol. Biol. Cell.* 3:475–479.

Hall, A. 1993. Ras-related proteins. *Curr. Opin. Cell Biol.* 5:265–268.

Heath, J. 1983. Behaviour and structure of the leading lamella in moving fibroblasts I. Occurrence and centripetal movement of arc-shaped microfilament bundles beneath the dorsal cell surface. *J. Cell Sci.* 60:331–354.

Herman, I. M. 1993. Actin isoforms. *Curr. Opin. Cell Biol.* 5:48–55.

Hiraoka, K., K. Kaibuchi, S. Ando, T. Musha, K. Takaishi, A. Mizuno, L. Menard, E. Tomhave, J. Didsbury, R. Snyderman, and Y. Takai. 1992. Both stimulatory and inhibitory GDP/GTP exchange proteins, smgGDS and rhoGDI, are active on multiple small GTP-binding proteins. *Biochem. Biophys. Res. Commun.* 182:921–930.

Kahn, R. A. 1991. Fluoride is not an activator of the smaller (20-25 kDa) GTP-binding proteins. *J. Biol. Chem.* 266:15595–15597.

Kawamoto, S., and H. Hidaka. 1984. 1-(5-Isoquinolinesulfonyl)-2-methylpiperazine (H-7) is a selective inhibitor of protein kinase C in rabbit platelets. *Biochem. Biophys. Res. Commun.* 125:258–264.

Koffer, A., A. J. Edgar, and J. R. Bamburg. 1988. Identification of two species of actin depolymerizing factor (ADF) in cultures of BHK cells. *J. Musc. Res. Cell Motil.* 9:320–328.

Koffer, A., and B. D. Gomperts. 1989. Soluble proteins as modulators of the

exocytotic reaction of permeabilized rat mast cells. *J. Cell Sci.* 94:585–591.
Koffer, A., P. E. R. Tatham, and B. D. Gomperts. 1990. Changes in the state of actin during the exocytotic reaction of permeabilized rat mast cells. *J. Cell Biol.* 111:919–927.
Koffer, A. 1993. Calcium induced secretion from permeabilized rat mast cells: requirements for guanine nucleotides. *Biochim. Biophys. Acta.* 1176:236–244.
Laemmli, U. K. 1970. Cleavage of structural proteins during the assembly of the head of bacteriophage T4. *Nature (Lond.).* 227:680–685.
Lassing, I., and U. Lindberg. 1988. Evidence that the phosphatidylinositol cycle is linked to cell motility. *Exp. Cell. Res.* 174:1–15.
Lillie, T. H. W., and B. D. Gomperts. 1993. Kinetic characterization of guanine nucleotide induced exocytosis from permeabilized rat mast cells. *Biochem. J.* 290:389–384.
Linstedt, A. D., and R. B. Kelly. 1987. Overcoming barriers to exocytosis. *Trends Neurosci.* 10:446–448.
Maciver, S., H. Zot, and T. Pollard. 1991. Characterization of actin filament severing by actophorin from *Acanthamoeba castellanii*. *J. Cell Biol.* 115:1611–1620.
Mousli, M., C. Bronner, Y. Landry, J. Bockaert, and B. Rouot. 1990. Direct activation of GTP-binding regulatory proteins (G-proteins) by substance P and compound 48/80. *FEBS (Fed. Eur. Biochem. Soc.) Lett.* 259:260–262.
Oberhauser, A. F., J. R. Monck, W. E. Balch, and J. M. Fernandez. 1992. Exocytotic fusion is activated by Rab3a peptides. *Nature (Lond.).* 360: 270–273.
Philips, M. R, S. B. Abramson, S. L. Kolasinski, K. A. Haines, G. Weissman, and M. G. Rosenfeld. 1991. Low molecular weight GTP-binding proteins in human neutrophil granule membranes. *J. Biol. Chem.* 266:1289–1298.
Pollard, T. D., and J. A. Cooper. 1986. Actin and actin-binding proteins. A critical evaluation of mechanisms and functions. *Annu. Rev. Biochem.* 55:987–1035.
Quinn, M., T. Evans, L. Loetterle, A. Jesaitis, and G. Bokoch. 1993. Translocation of rac correlates with NADPH oxidase activation. *J. Biol. Chem.* 268:20983–20987.
Ridley, A. J., and A. Hall. 1992. The small GTP-binding protein rho regulates the assembly of focal adhesions and actin stress fibers in response to growth factors. *Cell.* 70:389–399.
Ridley, A. J., H. F. Paterson, C. L. Johnston, D. Diekmann, and A. Hall. 1992. The small GTP-binding protein rac regulates growth factor-induced membrane ruffling. *Cell.* 70:401–410.
Sontag, J.-M., D. Aunis, and M.-F. Bader. 1988. Peripheral actin filaments control calcium-mediated catecholamine release from streptolysin-O-permeabilized chromaffin cells. *Eur. J. Cell Biol.* 46:316–326.
Stossel, T. P. 1989. From signal to pseudopod. *J. Biol. Chem.* 264:18261–18264.
Takai, Y., K. Kaibuchi, A. Kikuchi, and M. Kawata. 1992. Small GTP-binding proteins. *Int. Rev. Cytol.* 133:187–230.
Theriot, J, and T. Mitchison. 1992. The nucleation-release model of actin filament dynamics in cell motility. *Trends Cell Biol.* 2:219–221.
Therrien, S., and P. H. Naccache. 1989. Guanine nucleotide-induced polymerization of actin in electropermeabilized human neutrophils. *J. Cell Biol.* 109:1125–1132.
Yonezawa, N., E. Nishida, K. Iida, I. Yahara, and H. Sakari. 1990. Inhibitions of the interactions of cofilin, destrin and deoxyribonuclease I with actin by phosphoinositides. *J. Biol. Chem.* 265:8382–8386.
Zhang, J., W. King, S. Dillons, A. Hall, L. Feig, and S. Rittenhouse. 1993. Activation of platelet phosphatidylinositide 3-kinase requires the small GTP-binding protein rho. *J. Biol. Chem.* 268:22251–22254.